Physics and Imaging in Radiation Oncology 33 (2025) 100721

Contents lists available at ScienceDirect

Physics and Imaging in Radiation Oncology

journal homepage: www.sciencedirect.com/journal/physics-and-imaging-in-radiation-oncology

Original Research Article

Out-of-field dose assessment for pencil beam scanning proton radiotherapy versus photon radiotherapy for breast cancer in pregnant women

Menke Weessies *, Murillo Bellezzo, Britt J.P. Hupkens, Frank Verhaegen, Gloria Vilches-Freixas

Department of Radiation Oncology (Maastro) GROW School for Oncology and Reproduction Maastricht University Medical Centre Maastricht The Netherlands

ARTICLE INFO

Keywords:
Cancer during pregnancy
Out-of-field dosimetry
Fetus radiation
Proton radiation
Proton therapy
Radiation therapy

ABSTRACT

Background and purpose: Cancer affects 1 in 1000–2000 pregnancies annually worldwide, creating challenges in balancing cancer treatment and fetal safety. This study compares out-of-field radiation doses between two treatment modalities: 6MV external photon radiotherapy (XRT) and pencil beam scanning proton-therapy (PBS-PRT) for breast cancer, including imaging, to evaluate PBS-PRT as a potential new treatment option.
Materials and methods: For breast cancer involving lymph node levels 1–4 and the intramammary lymph nodes, treatment plans were created for XRT (with Flattening Filter (FF) and FF-Free (FFF)) and PBS-PRT, prescribing 15 × 2.67 Gy(RBE). Measurements were conducted using an adapted anthropomorphic phantom representing 20- and 30-week pregnancy. Bubble detectors placed in the phantom's abdomen assessed neutron dose from PBS-PRT, while a Farmer ion chamber was used for imaging and XRT dose.
Results: At 20 weeks, PBS-PRT including imaging delivered 22.4 mSv, reducing dose 3.4-fold versus 6FF XRT and 2.5-fold versus 6FFF XRT. At 30 weeks, the PBS-PRT dose was 25.4 mSv, resulting in 7.6-fold and 6.3-fold reductions compared to 6FF and 6FFF XRT, respectively.
Conclusions: This study presents the first one-by-one comparison between PBS-PRT and different XRT modalities for pregnant breast cancer patients with an adapted anthropomorphic phantom. PBS-PRT measurements showed that the total equivalent dose was below the 100 mSv threshold outlined in AAPM Task Group Report No. 36 for a 30-week pregnancy, even under a worst-case scenario, maintaining treatment goals. These findings support the adoption of PBS-PRT as the preferred approach for treating pregnant breast cancer patients, should radiotherapy be required.

1. Introduction

Cancer during pregnancy, affecting roughly 1 in 1000–2000 pregnancies globally every year, poses significant challenges in balancing maternal treatment and fetal protection [1–6]. Breast cancer is the most common malignancy in pregnancy, accounting for 39 % of cases [1,7]. With more women delaying pregnancy and cancer rates increasing with age, the incidence of cancer during pregnancy is expected to rise [8].

Cancer treatment during pregnancy involves experienced specialists following non-pregnant protocols as closely as possible while prioritizing the fetus's safety [9]. The use of chemotherapy during pregnancy is increasingly supported by research, with approximately half of pregnant patients undergoing this treatment. In contrast, radiation therapy use has declined, from 5 % of cases diagnosed before 2005 to 2 % after 2010, due to limited research on its safety [7]. Most data on prenatal irradiation effects come from studies of atomic bomb survivors, nuclear accidents, small study groups, and animal experiments [10,11]. Fetal radiation doses below 100 mSv are commonly assumed to be safe for deterministic effects at all stages of pregnancy [11–16]. However, the risk of stochastic effects, such as cancer and genetic impacts, is believed to increase linearly with dose, without a threshold, based on current evidence [17,18].

Pencil beam scanning (PBS) proton radiotherapy (PRT) is a promising alternative to photon radiation therapy (XRT) during pregnancy, offering better dosimetric characteristics and reducing normal tissue complications compared to passive scattering (PS) PRT and XRT [19]. However, PBS-PRT produces neutron-dominated out-of-field radiation, introducing dosimetry challenges associated with neutron detection. Neutrons transfer energy to protons and heavier ions, resulting in a high linear energy transfer (LET) and varying relative biological effectiveness (RBE) from 2 to 20 [20–23]. Estimating fetal radiation dose equivalent is challenging due to the mixed radiation environment. Furthermore,

* Corresponding author at: Doctor Tanslaan 12, 6229 ET Maastricht, The Netherlands.
E-mail address: menke.weessies@maastro.nl (M. Weessies).

https://doi.org/10.1016/j.phro.2025.100721
Received 1 October 2024; Received in revised form 29 January 2025; Accepted 31 January 2025
Available online 4 February 2025

neutron detectors vary in their energy-dependent response, combined with the broad energy spectrum of neutrons and sensitivity to various particles, complicating particle contributions [24].

Multiple case studies showed the feasibility of PBS-PRT during pregnancy [25–29]. Monte Carlo (MC) simulations show a ten-fold decrease in fetal exposure with PBS-PRT compared to XRT for various treatment sites [30,31]. However, most studies focus on active proton energy selection systems, with limited data available on PBS-PRT using a passive proton energy selection system, especially in the context of breast cancer and the impact of a growing abdomen on neutron dosimetry [26,28]. Secondly, Kry et al. demonstrated that flattening filter-free (FFF) deliveries consistently result in lower out-of-field dose, significantly reducing exposure outside the treatment volume [23].

This study aimed to explore the potential benefits of a passive energy selection PBS-PRT system using a modified "pregnant" phantom at 20 and 30 weeks of conceptional pregnancy, comparing the equivalent dose to the fetus to that of state-of-the-art (FF/FFF) XRT.

2. Methods and materials

2.1. Phantom

To represent a pregnant patient, we modified the female anthropomorphic Alderson Radiation Therapy phantom (RSD Radiology Support Devices, Long Beach, USA). The abdominal slices were replaced with 2.5 cm thick polymethyl methacrylate (PMMA) slices, which have a mass density of 1.18 g/cm^3 and a relative stopping power of 1.156 compared to water [32,33]. The design of the uniform PMMA slices and measurement locations was based on the hybrid computational pregnant female phantoms described by Maynard et al. and Lee et al. [34–36]. Two phantom versions were created to represent 20 and 30 weeks of conceptional pregnancy, as shown in Fig. 1.

The phantom used in this study features 2 cm diameter inserts designed to hold measurement detectors, with PMMA rods inserted when no detector was used. Insert 4 represents the uterine fundus at 20 weeks pregnancy, located 22.3 cm from the inferior edge of the clinical target volume (CTV), while insert 1 represents the uterine fundus at 30 weeks, 15.6 cm from the same point. This study focuses on the uterine fundus due to its proximity to the radiation field, a worst-case scenario.

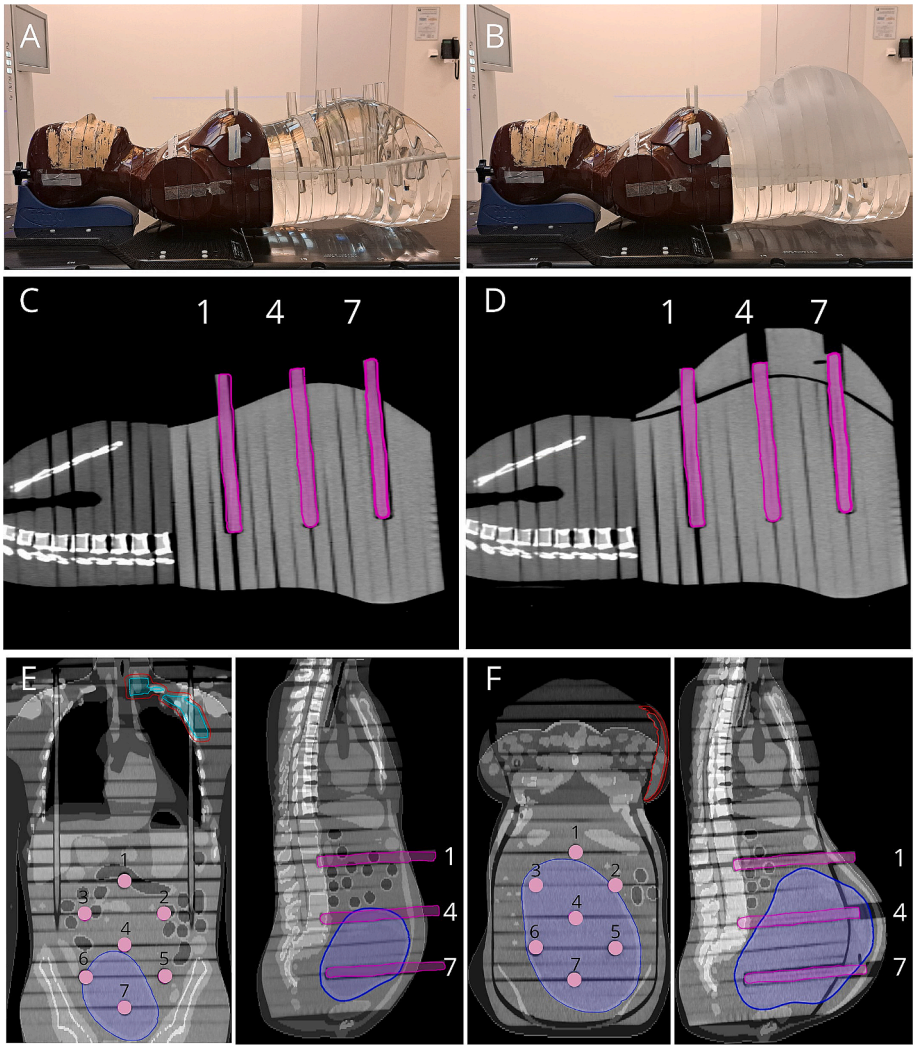

Fig. 1. A-B: The modified Alderson Radiation Therapy phantom including a representation of the abdominal region of a pregnant individual at 20 and 30 weeks of conceptional pregnancy, respectively. C-D: Sagittal cross-section of the Alderson Radiation Therapy phantom's thorax and abdomen at 20 and 30 weeks of pregnancy, respectively, with an axial slice thickness of 2.5 cm. E-F: Coronal and sagittal image fusion of the computational phantom of Lee et al. [36] and the PMMA phantoms used in this study highlights the regions where dose measurements are determined in relation to the anatomy. Different measurement inserts (1–7) are indicated in pink, the uterus in blue, partial view of the PTV in red, and partial view of the CTV, lymph node levels 1–4 in light blue. (For interpretation of the references to colour in this figure legend, the reader is referred to the web version of this article.)

However, since the fetal head shifts to a cephalic position later in pregnancy, its radiosensitivity must be considered in exposure assessments.

All inserts were used to measure the impact of anatomical changes at 30 weeks and estimate equivalent out-of-field (OoF) dose between 20 and 30 weeks. The CTV included the breast volume, lymph node levels 1–4, and the intramammary node. This phantom setup was used to estimate uterine fundus OoF-radiation dose in both PBS-PT and XRT plans, with imaging dose also evaluated for planning CT, setup kV X-rays, and cone beam CT (CBCT).

2.2. Imaging and irradiation systems

The planning Computed Tomography (CT) scans of the modified phantom were acquired using a Siemens SOMATOM Sensation Open CT (Siemens, Erlangen, Germany) with 120 kVp, 200 mAs, 3 mm slice thickness, and a High-Definition Field of View of 650 mm, with scan limits from vertebra C1 to include the lower part of the lungs.

The Varian TrueBeam STX linear accelerator (Varian Medical Systems, Palo Alto, CA), utilizing a 6 MV flattened (FF) beam for treatment and features a gantry-mounted onboard imager (OBI) for full rotation CBCT at 125 kVp with 268 mAs, and 2D kV X-ray imaging. This research also incorporates an FFF-system. The Halcyon™ Version 2.0 (Varian Medical Systems, Palo Alto, CA) uses an enclosed gantry, a 6 MV FFF beam for treatment and kV-imaging at 125 kVp and 101 mAs employing the thorax imaging protocol.

The nozzle of the Mevion S250i Hyperscan PBS-PRT system (Mevion Medical Systems, Littleton, MA) is equipped with a passive energy selection system that provides coverage across a broad range of depths, and an adaptive aperture (AA), which collimates the field laterally and energy-by-energy to improve the lateral penumbra [37]. It features two orthogonal flat panels and X-ray sources, utilizing settings of 70 kV and 4/40 mAs for 2D imaging and a CBCT system (Imaging Ring, medPhoton, Salzburg, Austria) utilizing 100 kV, 200 mAs and full-rotation protocol for 3D imaging.

2.3. Treatment plans

Two XRT treatment plans for the left breast were developed: a hybrid technique combining arcs and tangential beams for the Varian TrueBeam STX, and an IMRT technique for the Halcyon™ Version 2.0. The plans were delivered at a maximum dose rate of 600 MU/min with a nominal energy of 6 MV/6FFF. The setup and fractionation scheme (15x2.67 Gy(RBE)) remained unchanged, ensuring 95 % of the PTV received the full prescription dose (40.05 Gy) [38]. The CTV measured 380 cm^3, and the PTV was created by applying a 5 mm margin around the CTV.

An Intensity Modulated Proton Therapy (IMPT) PBS treatment plan for a Mevion S250i Hyperscan system, using a 15x 2.67 Gy(RBE) fractionation scheme, was created in RayStation 12A (RaySearch Laboratories, Stockholm, Sweden) with a Monte Carlo (MC) dose algorithm, Adaptive Aperture (AA) and robust optimization. The plan accounted for 1 % MC uncertainty, 5 mm setup uncertainty, and ± 3.0 % range uncertainty, using 10,000 protons per spot and a generic RBE of 1.1. A dual-isocenter plan with four beams at gantry angles of 0° and 45° was developed, with proton energies ranging from 36.3-134.1 MeV. CTV coverage quality was assessed through voxel-wise dose maps across 28 scenarios, ensuring robust coverage [39]. The treatment room dimensions were 6.43 × 5.48 × 3.20 m^3.

2.4. Dosimetry systems

For CT, kV-kV, and CBCT imaging and XRT OoF measurements, a PTW 0.6 cm^3 Farmer ion chamber (IC) type 30,001 (PTW, Freiburg, Germany) was used. The IC, with a buildup cap, was placed in different measurement positions (Fig. 1), it was calibrated for air kerma at 100 kV. Uncertainties of the Farmer measurements are 2.6 % (Supplementary material, Table S2). For the conversion from absorbed photon dose (D_t) to equivalent dose (H_t) in XRT, a radiation weighting factor (w_r) of 1 is used. For XRT, neutron production becomes significant only when beam energies exceed 8 MeV [40]. In this study, we exclusively used energies below 8 MeV; therefore, the neutron dose was not considered for XRT.

Bubble detectors designed for personal neutron dosimetry (Bubble Technology Industries, BTI, Chalk River, ON, Canada) were used to assess OoF neutron radiation. The detectors are calibrated against an Americium-Beryllium source. The Bubble Detectors for Personal Neutron Dosimetry (BD-PNDs) are sensitive to fast neutrons (>50 keV–15 MeV), while Bubble Detectors Thermal (BDTs) detect thermal and epithermal neutrons (~0.025 eV to ~1 eV). Two BD-PND sensitivities were employed, and the dose fraction was adjusted accordingly. After exposure, detectors were scanned using the X-RAD 225Cx micro-CT system (Precision X-Ray, 14 New Rd, Madison, CT, USA) with 0.1 mm resolution. A MATLAB script (The MathWorks, Inc., Natick, USA) automated bubble counting via thresholding techniques. Uncertainties for BD-PND (0.15bubbles(b)/μSv and 1.5b/μSv) and BDTs are 32.2 %, 33.2 %, and 34.2 % (k = 2), respectively, Supplementary material Table S1.

The bubble detector readings are in personal dose equivalent at 1 cm depth, $H_p(10)$ (mSv), with the detector having a volume of 6.4 cm^3. To determine the neutron dose equivalent in a point (H_i), we followed the methodology described by Romero-Expósito et al. [22]. In their methodology, Kerma factors (E) (mGy·cm^2) and quality factors $Q(E)$, specifically defined for ICRU reference tissues, were used [41,42]. They utilized these factors to determine a conversion factor with regards to the fluence and energy response of the bubble detectors. The conversion factor was determined to be 0.85 (BD-PND) and 1.0 (BDT) to convert the units from $H_p(10)$ (mSv) to neutron dose equivalent in a point (H_i) (mSv). The results were then summed accordingly [22,30,31,43].

The results are presented as an average over minimal 3 measurements per insert with uncertainties in percentage (k = 2). All treatment results are expressed in photon equivalent OoF-dose or neutron OoF-dose equivalent per prescription dose to the target (mSv/Gy(RBE)).

3. Results

3.1. Imaging equivalent dose

The equivalent OoF-dose per one CT and CBCT scan per distance to inferior edge of the imaging field in cm is shown in Table 1 and Fig. 2. For a pair of 2D x-ray images, the equivalent OoF-dose ranged from < 0.5–13 μSv.

3.2. Out of field dose from treatment plans

Fig. 3 illustrates the photon equivalent OoF-dose or neutron OoF-dose equivalent estimates at the uterine fundus from XRT and PBS-PRT treatment plans. These estimates were based on the distance from the inferior edge of the CTV to the detector per Gy(RBE) treatment dose at the target, evaluated for 20- and 30-week pregnant phantoms. The impact of a growing belly at 30 weeks and OoF-dose estimates are detailed in the Supplementary material S3. In the PBS plan, the fast neutron dose equivalent for the 20-week averaged 0.52 mSv/Gy(RBE) at 22.3 cm (insert 4), and 0.56 mSv/Gy(RBE) for the 30-week at 15.6 cm (insert 1). The thermal neutron dose equivalent reached a maximum of 0.03 mSv/Gy(RBE) for both pregnancy stages, with the total shown in Table 2.

4. Discussion

This study demonstrated that PBS-PRT significantly reduced fetal radiation exposure compared to both 6FF and 6FFF XRT, with doses well

Table 1
Photon equivalent dose determined in the conceptional 20- and 30-weeks pregnant phantoms from the CT scan, CBCT TrueBeam, CBCT Halcyon and CBCT Imaging Ring at different distances. Abbreviations: CBCT = Cone Beam CT, SD = Standard Deviation, OoF = Out Of Field.

Conceptional Age (weeks)	Insert	Distance to inferior edge of the imaging field (cm)	X-ray imaging OoF-dose (mSv) (SD)			
			Somatom CT	TrueBeam CBCT	Halcyon CBCT	Imaging Ring CBCT
20	4	17.5	0.23 (0.01)	0.24 (0.01)	0.09 (<0.01)	0.04 (<0.01)
30	1	7.5	1.05 (0.03)	0.68 (0.02)	0.16 (<0.01)	0.2 (0.01)

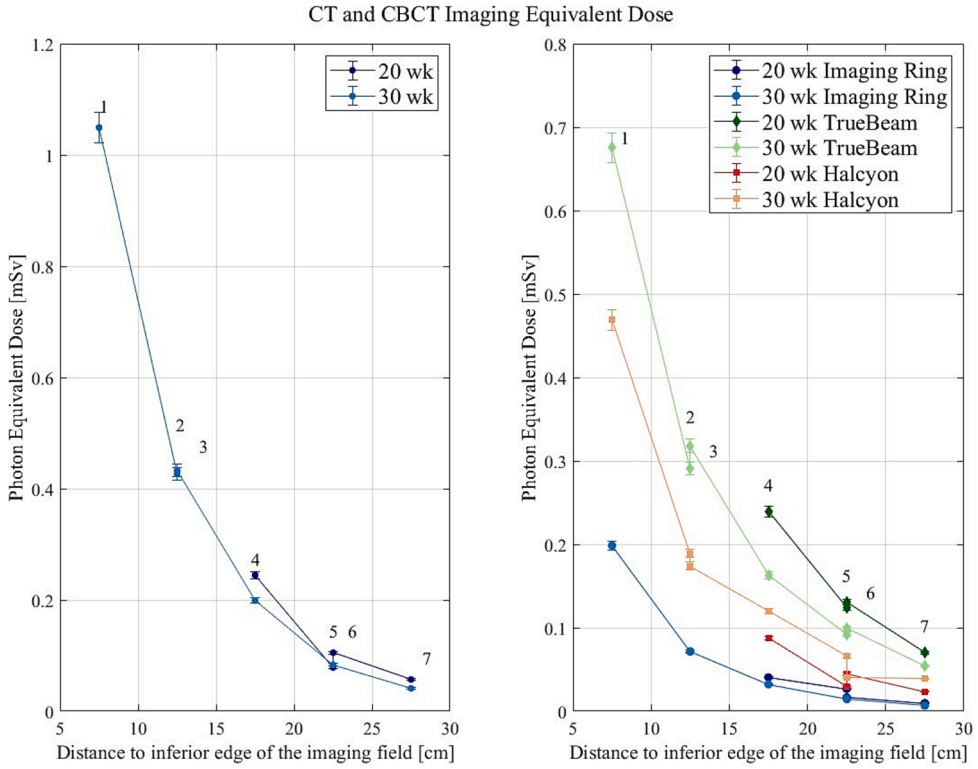

Fig. 2. (left): Average photon equivalent OoF-dose per insert from the CT scan, determined using the Farmer IC detector, with the conceptional 20- and 30-week pregnant phantom at different distances from the imaging field edge. The numbers indicated correspond to the insert numbers in Fig. 1b. Fig. 2 (right): Average photon equivalent dose per insert from the different CBCTs (TrueBeam, Halcyon, and Imaging Ring systems), determined using the Farmer IC, with the conceptional 20- and 30-week pregnant phantom, at different distances from the imaging field edge. The numbers indicated correspond to the insert numbers in Fig. 1b.

below the 100 mSv safety threshold. At 20 weeks, the OoF-dose was 22.4 mSv, a 3.4-fold and 2.5-fold reduction compared to 6FF and 6FFF XRT, respectively. At 30 weeks the PBS-PRT OoF-dose increased to 25.42 mSv but still achieved 7.6-fold and 6.3-fold reductions.

The customized phantom was designed and produced for this study, whereas other studies often add additional materials, such as Lucite, gelatin, wax, or polyurethane resin, on top of a phantom's pelvis [44–46]. This study opted to replace the entire pelvis with PMMA. Individualized pregnant phantoms can be 3D-printed, but this time-intensive process is impractical giving the rapidly changing patient anatomy during pregnancy [47].

This study assessed X-ray imaging OoF-doses using Farmer IC detector, which was calibrated in terms of air kerma at 100 kV. For conservative estimates, weekly CT verification scans during PBS-PT are estimated to deliver a maximum equivalent OoF-dose of 1.1 mSv per scan at the uterine fundus. While CBCT typically delivers a lower equivalent OoF-dose than CT, its usage for several fractions significantly increases exposure. CT scans demonstrate a fivefold dose reduction between inserts 1 and 4, while CBCT show a more gradual dose fall-off, indicating lower dose attenuation. Although CBCT-systems have broader beams and less collimation, conventional CT-scanners achieve steeper dose fall-off outside the primary field due to advanced collimation and scatter reduction techniques.

However, imaging parameters like scan range, beam current, field size and voltage significantly affects CBCT dose in- and out-field [48–53]. Careful consideration and precautions are crucial when using CBCT on pregnant patients. The 2D imaging doses for XRT on TrueBeam and Mevion systems yield just 0.013 mSv per image pair, making it a preferred option for matching the anatomy of the patient during treatment. Additionally, incorporating surface-guided RT enhances positioning accuracy in breast radiotherapy, ensuring safety for both the fetus and the patient. It could be considered to combine these techniques [54].

For 6FF XRT, treating breast cancer patients beyond 20 weeks of pregnancy poses significant risks due to high total equivalent OoF-dose. At 30 weeks, the equivalent OoF-dose reaches 190.8 mSv, and at 20 weeks, 74.5 mSv for a 40.05 Gy prescription, excluding imaging. Shielding was omitted because, even with an anticipated 40 % reduction from collimator and flattening filter scatter, the total equivalent OoF-dose was still expected to exceed the 100 mSv threshold [11,23]. Consequently, maintaining the OoF-dose below 100 mSv at 30 weeks with 6FF XRT is unfeasible (see Table 3). Conversely, 6FFF XRT reduces OoF-dose by 30 % compared to 6FF XRT, making it a viable backup for PBS-PRT. The data shows a notable variation between inserts 3 and 4, likely caused by differences in distance to the linac head, where head-scatter significantly contributes to the measured dose [23].

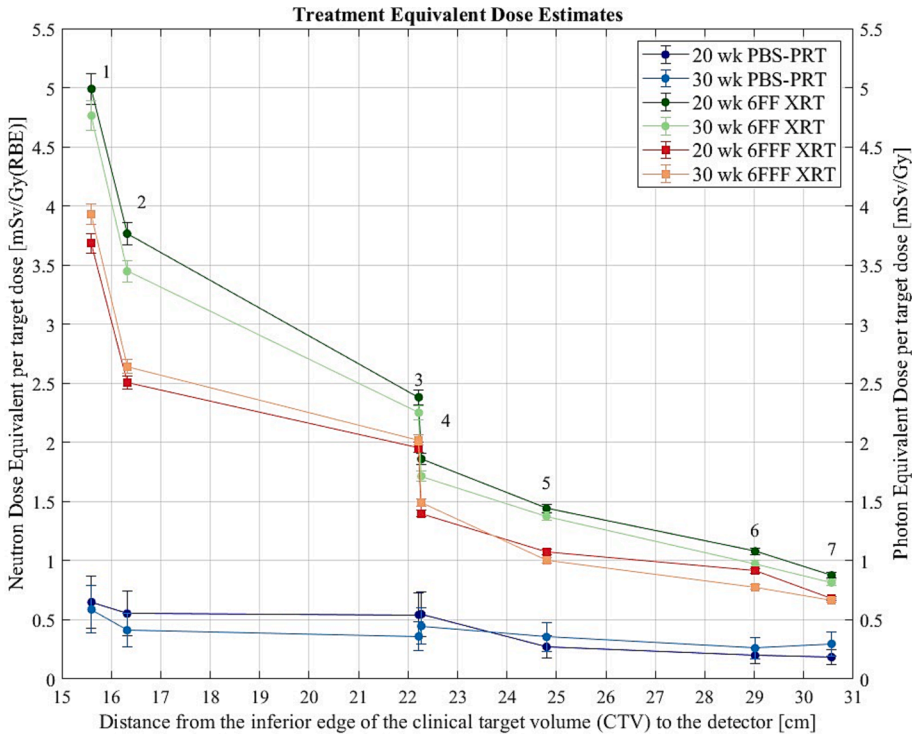

Fig. 3. The total average photon equivalent OoF-dose or summed thermal and fast neutron OoF-dose equivalent estimates from 6FF XRT, 6FFF XRT and PBS-PRT plans as a function of distance from the inferior edge of the CTV to the detector for the 20 and 30-week conceptional age phantoms. The error bars represent the uncertainty from the detectors. The indicated numbers are the insert numbers in Fig. 1b.

Table 2
Average photon equivalent OoF-dose or neutron OoF-dose equivalent estimates from 6FF XRT, 6FFF XRT and PBS-PRT plans at various distances to the detector. Abbreviations: XRT = Photon Radiotherapy, PBS – PRT = Pencil Beam Scanning Proton Therapy, SD = Standard Deviation, OoF = Out Of Field.

Conceptional Age (weeks)	Distance to inferior edge of the CTV to detector (cm)	Photon equivalent OoF-dose(mSv/Gy) (SD)		Neutron OoF-dose equivalent(mSv/Gy(RBE)) (SD)
		6FF XRT	6FFF XRT	PBS – PRT
20	22.3	1.86 (0.05)	1.4 (0.04)	0.55 (0.18)
30	15.6	4.76 (0.12)	3.9 (0.10)	0.59 (0.19)

Table 3
The total average photon equivalent OoF-dose from the 6FF XRT and 6FFF XRT plans or neutron OoF-dose equivalent estimates from PBS-PRT treatment plan, including imaging dose per conceptional age. In parenthesis the standard deviation (see Supplementary material S1 and S2). Abbreviations: XRT = Photon Radiotherapy, PBS – PRT = Pencil Beam Scanning Proton Therapy, SD = Standard Deviation, OoF = Out Of Field, CBCT = Cone Beam CT.

Treatment	Conceptional age (weeks)	CT (#)	CBCT (#)	2D x-ray images (#)	OoF dose (mSv) (SD)	Total OoF-dose (mSv) (SD)
6FFF XRT	20	1	15	0	56.1 (1.6)	57.7 (1.6)
	30	1	15	0	157.6 (4.0)	160.9 (4.0)
6FF XRT	20	1	3	12	74.5 (2.0)	75.6 (2.0)
	30	1	3	12	190.6 (4.8)	199.7 (4.8)
PBS-PRT	20	3	15	0	21.9 (7.2)	23.2 (7.2)
	30	3	15	0	23.5 (7.6)	30.0 (7.6)
PBS-PRT	20	1	3	12	21.9 (7.2)	22.4 (7.2)
	30	1	3	12	23.5 (7.6)	25.4 (7.6)

In comparison with our PBS-PRT findings a study measured a maximum fetal dose of 64.7 μSv/2Gy(RBE) at 43.5 cm for a brain lesion using the Mevion S250i system also with a dynamic aperture [26]. Dupere et al. using a different PBS-PRT system reported fetal equivalent dose of 0.007 mSv/Gy(RBE) at 40 cm and 0.19 mSv/Gy(RBE) at 25 cm for brain plans and head and neck plans, excluding the imaging dose [55]. Another study, measured fetal dose of 0.06, 0.04, and 0.01 mSv/Gy(RBE) at 30, 40, and 50 cm, respectively during IMPT for a pregnant patient with astrocytoma, with similar neutron contributions [56]. Our study found, three times higher dose: 0.18 mSv/Gy(RBE) at 30.6 cm. Heimovaara et al. observed an ambient dose equivalent of 0.06 mSv/Gy (RBE) at 20 cm for a pregnant nasopharyngeal carcinoma patient undergoing IMPT with an IBA system [57]. These studies used the WENDI-II detector to measure neutron dose equivalent. However, due to the pulsed nature of the Mevion S250i makes the detector unsuitable due to pile-up and saturation effects [24]. Therefore, we used bubble detectors, though their sensitivity to charged particles may affect accuracy. Knežević et al. demonstrated that neutron dose dominates beyond 12 cm from the field edge [58]. As our measurements were taken at 15.6 cm, overestimation is expected to be minimal due to minimal scattered protons.

It is important to note that BDTs and BD-PNDs have an uncertainty related to their energy response above 20 MeV. High-energy protons can induce nuclear reactions within beam-shaping elements (such as range shifters (RS)) or within the patient, resulting in the generation of secondary neutrons. In the Mevion S250i system, passive energy

modulation employs ~227 MeV protons, which pass through the RS and produce neutrons predominantly emitted in the forward beam direction due to momentum transfer and relativistic Lorentz boosting [59–61]. However, in this study, our measurement positions were outside the beam field. The majority of neutrons in the OoF-range are anticipated in the evaporation stage, characterized by an isotropic angular distribution and energies around 1 MeV [61]. This isotropic distribution may explain the step observed at ±22 cm in our data (Fig. 3). The discrepancy likely results from two different inserts at similar distances but different positions relative to the CTV. The tumor was located on the left side, while inserts 3 and 4—both approximately 22.5 cm away—were on the right and in the middle of the phantom, respectively. This suggests that, unlike XRT, neutron fluence or dose, is influenced not only by distance but also by the neutron production direction and the intervening materials.

Additionally, the BDT's manufacturer reports a sensitivity ratio to fast neutrons of 1:10, possibly overestimating thermal neutron dose. Since, thermal neutrons contribute less than 1 % to the overall dose, and Van Havere et al. found the BDT's response to thermal neutrons is 19.3 times higher than to fast neutrons, we made no correction for this minor overestimation [24,43,62].

Despite uncertainties, BD-PNDs and BDTs have shown strong agreement with MC simulations [56,62–64]. Wochnik et al., used bubble detectors to estimate neutron dose equivalents (H_i) at various distances from the isocenter, reporting 0.195, 0.057 and 0.030 mSv/Gy(RBE) at 13, 20, and 32 cm, respectively [59]. Other studies using passive detectors, such as polyallyl-diglycol carbonate (PADC) track detectors, reported neutron equivalent doses decreasing from 0.15-0.2 mSv/Gy (RBE) at 18 cm to 0.014–0.15 mSv/Gy(RBE) at 23 cm, approximately half of our results [65]. This discrepancy could be attributed by studies showing a 30 % increase in neutron production when a RS is used in a PBS-RT plan compared to plans without it [24,55]. The Mevion S250i Hyperscan system requires a passive energy modulation with various RS plate combinations to generate proton energies, increasing neutron production. Given the superficial location of the CTV target in breast cancer and the typical PBS minimum energy in cyclotron facilities (60–100 MeV), a RS is necessary to achieve the lower energies required for adequate target coverage in all commercial PBS systems with active energy modulation.

While this study does not address the gamma contribution to the out-of-field dose in PBS-RT, literature reports this as ~0.008 mSv/Gy at 15 cm from the field edge [22]. For a 40.05 Gy treatment, this equates to 0.32 mSv, a measurable but negligible contribution.

Recent literature increasingly addresses OoF-doses for pregnant patients. Based on these factors, we recommend PBS-PRT as the preferred treatment for pregnant breast cancer patients. However, it is crucial to recognize that not all PBS-PRT systems are identical, and factors such as the use of a RS and the distance to the fetus play significant roles. Despite uncertainties, this study demonstrated that even with a passive energy modulation PBS-system, the OoF-dose from PBS-PRT is approximately 4–8 times lower than XRT, staying within the TG-36 safety limit for pregnant patients [11].

Declaration of competing interest

The authors declare that they have no known competing financial interests or personal relationships that could have appeared to influence the work reported in this paper.

Appendix A. Supplementary data

Supplementary data to this article can be found online at https://doi.org/10.1016/j.phro.2025.100721.

References

[1] Haas JF. Pregnancy in association with a newly diagnosed cancer: a population-based epidemiologic assessment. Int J Cancer Res 1984;34:229–35. https://doi.org/10.1002/ijc.2910340214.

[2] Eibye S, Kjaer SK, Mellemkjaer L. Incidence of pregnancy-associated cancer in Denmark, 1977-2006. Obstet Gynecol 2013;122:608–17. https://doi.org/10.1097/AOG.0b013e3182a057a2.

[3] Stensheim H, Moller B, van Dijk T, Fossa SD. Cause-specific survival for women diagnosed with cancer during pregnancy or lactation: a registry-based cohort study. J Clin Oncol 2009;27:45–51. https://doi.org/10.1200/JCO.2008.17.411.

[4] Donegan WL. Cancer and pregnancy. CA 1983;33:194–214. https://doi.org/10.3322/canjclin.33.4.194.

[5] Peccatori FA, Azim HA, Orecchia R, Hoekstra HJ, Pavlidis N, Kesic V, et al. Cancer, pregnancy and fertility: ESMO Clinical Practice Guidelines for diagnosis, treatment and follow-up. Ann Oncol 2013;24:vi160–70. https://doi.org/10.1093/annonc/mdt199.

[6] Silverstein J, Post AL, Chien AJ, Olin R, Tsai KK, Ngo Z. Multidisciplinary management of cancer during pregnancy. JCO Oncol Pract 2020;16:545–57. https://doi.org/10.1200/OP.20.00077.

[7] De Haan J, Verheecke M, Van Calsteren K, Van Calster B, Shmakov RG, Mhallem Gziri M, et al. Oncological management and obstetric and neonatal outcomes for women diagnosed with cancer during pregnancy: a 20-year international cohort study of 1170 patients. Lancet Oncol 2018;19:337–46. https://doi.org/10.1016/S1470-2045(18)30059-7.

[8] Amant F, Loibl S, Neven P, Van Calsteren K. Breast cancer in pregnancy. Lancet 2012;379:570–1559. https://doi.org/10.1016/S0140-6736(11)61092-1.

[9] Amant F, Deckers S, Van Calsteren K, Loibl S, Halaska M, Brepoels L, et al. Breast cancer in pregnancy: recommendations of an international consensus meeting. Eur J Cancer 2010;46:3158–68. https://doi.org/10.1016/j.ejca.2010.09.010.

[10] Schull WJ. Effects of atomic radiation. A half-century of studies from Hiroshima and Nagasaki. New York: Wiley-Liss; 1995. 10.1126/science.272.5269.1748.

[11] Stovall M, Blackwell CR, Cundiff J, Shalek RJ, et al. Fetal dose from radiotherapy with photon beams: Report of AAPM Radiation Therapy Committee Task Group No. 36. Med Phys 1995;22:63–82. https://doi.org/10.1118/1.597525.

[12] Fattibene P, et al. Prenatal exposure to ionizing radiation: sources, effects, and regulatory aspects. Acta Paediatr 1999;88:693–702. https://doi.org/10.1111/j.1651-2227.1999.tb00024.x.

[13] Kal HB, Struikmans H. Radiotherapy during pregnancy: fact and fiction. Lancet Oncol 2005;6:328–33. https://doi.org/10.1016/S1470-2045(05)70169-8.

[14] Otake M, Schull WJ, Fujikoshi Y, Yoshimaru H. Effect on school performance of prenatal exposure to ionizing radiation in Hiroshima: a comparison of the T65DR and DS86 dosimetry systems. RERF TR No. 2-88. 1988. PMID: 1956123 https://doi.org/10.1265/jjh.46.747.

[15] Otake M. Threshold for radiation-related severe mental retardation in prenatally exposed A-bomb survivors: a re-analysis. Int J Radiat Biol 1996;70:755–63. https://doi.org/10.1080/09553096144644.

[16] Doll R, Wakeford R. Risk of childhood cancer from fetal irradiation. Br J Radiol 1997;70:130–9. https://doi.org/10.1259/bjr.70.830.9135438.

[17] Streffer C, Shore R, Konermann G, Meadows A, Uma Devi P, Preston Withers J, et al. Biological effects after prenatal irradiation (embryo and fetus). Ann ICRP 2003;33:5–206. PMID: 12963090.

[18] ICRP. 1990 Recommendations of the International Commission on Radiological Protection. Ann ICRP 1991;21(1–3). https://doi.org/10.1093/oxfordjournals.rpd.a032030.

[19] Newhauser WD, Zhang R. The physics of proton therapy. Phys Med Biol 2015;60:R155. https://doi.org/10.1088/0031-9155/60/8/R155.

[20] Butterworth KT, McGarry CK, Clasie B, Carabe-Fernandez A, Schuemann J, Depauw N, et al. Relative biological effectiveness (RBE) and out-of-field cell survival responses to passive scattering and pencil beam scanning proton beam deliveries. Phys Med Biol 2012;57:6671–85. https://doi.org/10.1088/0031-9155/57/20/6671.

[21] Cameron J. The relative biological effectiveness of radiations of different quality, NCRP Report 104. 1992. https://doi.org/10.2307/3578145.

[22] Romero-Expósito M, Domingo C, Sánchez-Doblado F, Ortega-Gelabert O, Gallego S. Experimental evaluation of neutron dose in radiotherapy patients: which dose? Med Phys 2016;43:360–77. https://doi.org/10.1118/1.4938578.

[23] Kry SF, Bednarz B, Howell RM, Dauer L, Followill D, Klein E, et al. AAPM TG 158: Measurement and calculation of doses outside the treated volume from external-beam radiation therapy. Med Phys 2017;44:e391–429. https://doi.org/10.1002/mp.12462.

[24] Zorloni G, Bosmans G, Brall T, et al. Joint EURADOS WG9-WG11 rem-counter intercomparison in a Mevion S250i proton therapy facility with Hyperscan pulsed synchrocyclotron. Phys Med Biol 2022;67:075005. https://doi.org/10.1088/1361-6560/ac5b9c.

[25] Blommaert J, De Saint-Hubert M, Depuydt T, et al. Challenges and opportunities for proton therapy during pregnancy. Acta Obstet Gynecol Scand 2023. https://doi.org/10.1111/aogs.14645.

[26] Hopfensperger KM, Li X, Paxton A, et al. Measurements of fetal dose with Mevion S250i proton therapy system with HYPERSCAN. J Appl Clin Med Phys 2023. https://doi.org/10.1002/acm2.13957.

[27] Le Guevelou J, Trompier F, Villagrasa C, et al. Measurement of out-of-field dose to the uterus during proton therapy of the head and neck. Cancer Radiother 2020;24:138–42. https://doi.org/10.1016/j.canrad.2019.10.004.

[28] Kalbasi A, Kirk M, Teo BKK, et al. Proton craniospinal irradiation during the third trimester of pregnancy. Pract Radiat Oncol 2018;8:213–6. https://doi.org/10.1016/j.prro.2017.09.005.
[29] Wang X, Poenisch F, Sahoo N, et al. Spot scanning proton therapy minimizes neutron dose in the setting of radiation therapy administered during pregnancy. J Appl Clin Med Phys 2016;17:366–76. https://doi.org/10.1120/jacmp.v17i5.6327.
[30] Geng C, Moteabbed M, Seco J, et al. Dose assessment for the fetus considering scattered and secondary radiation from photon and proton therapy when treating a brain tumor of the mother. Phys Med Biol 2016;61:683–95. https://doi.org/10.1088/0031-9155/61/2/683.
[31] Saint-Hubert D, Verbeek N, Bäumer C, Esser J, Wulff J, Nabha R, et al. Validation of a Monte Carlo framework for out-of-field dose calculations in proton therapy. Front Oncol 2022;12:882489. https://doi.org/10.3389/fonc.2022.882489.
[32] Parodi K, Ponisch F, Enghardt W. Experimental study on the feasibility of in-beam PET for accurate monitoring of proton therapy. IEEE Trans Nucl Sci 2005;52:778–86. https://doi.org/10.1109/tns.2005.850950.
[33] Dowdell S, Clasie B, Wroe A, Guatelli S, Metcalfe P, Schulte R, et al. Tissue equivalency of phantom materials for neutron dosimetry in proton therapy. Med Phys 2009;36:5412–9. https://doi.org/10.1118/1.3250857.
[34] Maynard MR, Long NS, Moawad NS, Shifrin RY, Geyer AM, Fong G, et al. The UF family of hybrid phantoms of the pregnant female for computational radiation dosimetry. Phys Med Biol 2014;59:4325–42. https://doi.org/10.1088/0031-9155/59/15/4325.
[35] Lee C, Lodwick D, Hurtado J, Pafundi D, Williams JL, Bolch WE. The UF family of reference hybrid phantoms for computational radiation dosimetry. Phys Med Biol 2010;55:339–63. https://doi.org/10.1088/0031-9155/55/2/002.
[36] Lee C, Jung JW, Pelletier C, Pyakuryal A, Lamart S, Kim JO, et al. Reconstruction of organ dose for external radiotherapy patients in retrospective epidemiologic studies. Phys Med Biol 2015;60:2309–24. https://doi.org/10.1088/0031-9155/60/6/2309.
[37] Vilches-Freixas G, Unipan M, Rinaldi IP, Bosmans G. Beam commissioning of the first compact proton therapy system with spot scanning and dynamic field collimation. Br J Radiol 2020;93:20190598. https://doi.org/10.1259/bjr.20190598.
[38] Boere I, Lok C, Poortmans P, Koppert L, vd Heuvel-Eibrink MM, Amant F. Breast cancer during pregnancy: epidemiology, phenotypes, presentation during pregnancy and therapeutic modalities. Best Pract Res Clin Obstet Gynaecol 2022. https://doi.org/10.1016/j.bpobgyn.2022.05.001.
[39] Korevaar EW, Habraken SJ, Unipan M, Eenink MG, Langendijk JA. Practical robustness evaluation in radiotherapy–a photon and proton-prOoF alternative to PTV-based plan evaluation. Radiother Oncol 2019;141:267–74. https://doi.org/10.1016/j.radonc.2019.08.005.
[40] Zanini A, Durisi E, Fasolo F, Ongaro C, Visca L, Nastasi U, et al. Monte Carlo simulation of the photoneutron field in linac radiotherapy treatments with different collimation systems. Phys Med Biol 2004;49:571–82. https://doi.org/10.1088/0031-9155/49/4/008.
[41] Siebert BRL, Schuhmacher H. Quality factors, ambient and personal dose equivalent for neutrons, based on the new ICRU stopping power data for protons and alpha particles. Radiat Prot Dosimetry 1995;58:177–83. https://doi.org/10.1093/oxfordjournals.rpd.a082612.
[42] Chadwick MB, Barschall HH, Caswell RS, DeLuca PM, Hale GM, Jones DTL, et al. A consistent set of neutron kerma coefficients from thermal to 150 MeV for biologically important materials. Med Phys 1999;26:974–91. https://doi.org/10.1118/1.598601.
[43] Vanhavere F, Loos M, Plompen AJM, Wattecamps E, Thierens H. A combined use of the BD-PND and BDT bubble detectors in neutron dosimetry. Radiat Meas 1998;29:573–7. https://doi.org/10.1016/S1350-4487(98)00071-7.
[44] Solomou G, Papadakis AE, Damilakis J. Abdominal CT during pregnancy: A phantom study on the effect of patient centring on conceptus radiation dose and image quality. Eur Radiol 2014;25:911–21. https://doi.org/10.1007/s00330-014-3505-2.
[45] Saeed MK. Comparison of estimated and calculated fetal radiation dose for a pregnant woman who underwent computed tomography and conventional X-ray examinations based on a phantom study. Radiol Phys Technol 2021;14:25–33. https://doi.org/10.1007/s12194-020-00598-9.
[46] Matsunaga Y, Haba T, Kobayashi M, Suzuki S, Asada Y, Chida K. Fetal radiation dose of four tube voltages in abdominal CT examinations during pregnancy: a phantom study. J Appl Clin Med Phys 2021;22:178–84. https://doi.org/10.1002/acm2.13171.
[47] Kunert P, Schlattl H, Trinkl S, Honorio da Silva E, Reichert D, Giussani A. 3D printing of realistic body phantoms: comparison of measured and simulated organ doses on the example of a CT scan on a pregnant woman. Med Phys 2024. https://doi.org/10.1002/mp.17420.
[48] Perks JR, Lehmann J, Chen AM, Yang CC, Stern RL, Purdy JA. Comparison of peripheral dose from image-guided radiation therapy (IGRT) using kV cone beam CT to intensity-modulated radiation therapy (IMRT). Radiother Oncol 2008;89:304–10. https://doi.org/10.1016/j.radonc.2008.07.026.
[49] Kan MW, Leung LH, Wong W, Lam N. Radiation dose from cone beam computed tomography for image-guided radiation therapy. Int J Radiat Oncol Biol Phys 2008;70:272–9. https://doi.org/10.1016/j.ijrobp.2007.08.062.
[50] Song WY, Kamath S, Ozawa S, Al Ani S, Chvetsov A, Bhandare N, et al. A dose comparison study between XVI® and OBI® CBCT systems. Med Phys 2008;35:480–6. https://doi.org/10.1118/1.2825619.
[51] Onozato Y, Kadoya N, Fujita Y, Arai K, Dobashi S, Takeda K, et al. Evaluation of on-board kV cone beam CT-based dose calculation using deformable image registration and modification of HU values. Int J Radiat Oncol Biol Phys 2013;87:S711–2. https://doi.org/10.1016/j.ijrobp.2014.02.007.
[52] Olch AJ, Alaei P. How low can you go? a CBCT dose reduction study. J Appl Clin Med Phys 2021;22:85–9. https://doi.org/10.1002/acm2.13164.
[53] Agnew CE, McCallum C, Johnston G, Workman A, Irvine DM. Optimisation of Varian TrueBeam head, thorax and pelvis CBCT based on patient size. J Radiother Pract 2021;20:248–56. https://doi.org/10.1017/S1460396920000618.
[54] González-Sanchis A, Brualla-González L, Fuster-Diana C, et al. Surface-guided radiation therapy for breast cancer: more precise positioning. Clin Transl Oncol 2021;23:2120–6. https://doi.org/10.1007/s12094-021-02617-6.
[55] Dupere JM, Lucido JJ, Breen WG, et al. Pencil beam scanning proton therapy for pregnant patients with brain and head and neck cancers. Int J Radiat Oncol Biol Phys 2024;118:853–8. https://doi.org/10.1016/j.ijrobp.2023.09.040.
[56] Rahimi R, Taylor M, Li X, et al. Fetal dose assessment in a pregnant patient with brain tumor: a comparative study of proton PBS and 3DCRT/VMAT radiation therapy techniques. J Appl Clin Med Phys 2024. https://doi.org/10.1002/acm2.14394.
[57] Heimovaara JH, Blommaert J, Free J, Bolt RA, Gort EM, Depuydt T, et al. Proton therapy of a pregnant patient with nasopharyngeal carcinoma. Clin Transl Radiat Oncol 2022;35:33–6. https://doi.org/10.1016/j.ctro.2022.04.014.
[58] Knežević Ž, Stolarczyk L, Ambrožová I, Caballero-Pacheco MA, Davídková M, De Saint-Hubert M, et al. Out-of-field doses produced by a proton scanning beam inside pediatric anthropomorphic phantoms and their comparison with different photon modalities. Front Oncol 2022;12:904563. https://doi.org/10.3389/fonc.2022.904563.
[59] Englbrecht FS, Trinkl S, Mares V, et al. A comprehensive Monte Carlo study of out-of-field secondary neutron spectra in a scanned-beam proton therapy gantry room. Z Med Phys 2021;31:215–28. https://doi.org/10.1016/j.zemedi.2021.01.001.
[60] Geser FA, Stabilini A, Christensen JB, et al. A Monte Carlo study on the secondary neutron generation by oxygen ion beams for radiotherapy and its comparison to lighter ions. Phys Med Biol 2024;69:015027. https://doi.org/10.1088/1361-6560/ad0f45.
[61] Vedelago J, Schmidt S, Stengl C, Karger CP, Jäkel O. Secondary neutrons in proton and light ion beam therapy: A review of current status, needs and potential solutions. Radiat Meas 2024. https://doi.org/10.1016/j.radmeas.2024.107214.
[62] De Saint-Hubert M, Saldarriaga Vargas C, Van Hoey O, et al. Secondary neutron doses in a proton therapy centre. Radiat Prot Dosimetry 2016;170:336–41. https://doi.org/10.1093/rpd/ncv458.
[63] Knežević Ž, Ambrozova I, Domingo C, et al. Comparison of response of passive dosimetry systems in scanning proton radiotherapy—a study using paediatric anthropomorphic phantoms. Radiat Prot Dosimetry 2018;180:256–60. https://doi.org/10.1093/rpd/ncx254.
[64] Colson D, Blommaert J, Poels K, et al. Extended in-field and out-of-field validation of a compact Monte Carlo model of an IBA PROTEUS® ONE proton beam in TOPAS/GEANT4. Phys Med Biol 2023;68:21NT02. https://doi.org/10.1088/1361-6560/ad03a9.
[65] Wochnik A, Stolarczyk L, Ambrožová I, et al. Out-of-field doses for scanning proton radiotherapy of shallowly located paediatric tumours—a comparison of range shifter and 3D printed compensator. Phys Med Biol 2021;66:035012. https://doi.org/10.1088/1361-6560/abcb1f.